# SURFACE VIBRATIONAL SPECTROSCOPY

J. L. Erskine
Department of Physics
University of Texas
Austin, Texas 78712

ABSTRACT

A brief review of recent studies which combine measurements of surface vibrational energies with lattice dynamical calculations is presented. These results suggest that surface vibrational spectroscopy offers interesting prospects for use as a molecular-level probe of surface geometry, adsorbate bond distances and molecular orientations.

## I. Introduction

High-resolution electron energy loss spectroscopy (EELS) is rapidly being developed into one of the most useful techniques for probing physical and chemical phenomena at surfaces. EELS is based on detection of quantum energy losses (or gains) in a monoenergetic electron beam scattered from a surface. Due to the short mean free path of low-energy electrons in solids, the quantum energy losses result primarily from intrinsic surface vibrations (surface phonons) or vibrations of adsorbed surface atoms or molecules. The technique offers high surface sensitivity (.001 monolayer in ideal cases) with a broad spectral range (good spectrometers can detect losses below 20 meV).

Recent work which combines vibrational energies determined using EELS with lattice dynamical calculations has suggested that surface vibrational spectroscopy offers interesting prospects for testing surface structural models. EELS studies of O/Al(111)[1] combined with lattice dynamical calculations[2] have shown that surface complexes consisting of both overlayer and underlayer chemisorbed species can be investigated using inelastic electron scattering. Similar investigations of O/Ni(100)[3-6] have shown that EELS can be used to test

structural models and adsorbate bond distances. This paper briefly reviews the pertinent studies which combine EELS and lattice dynamical calculations to address issues related to the structure and bond distances at surfaces.

## II. Electron Scattering at Surfaces

A single spectroscopic technique dominates studies of the bulk vibrational properties of solids (neutron scattering) and of gas-phase molecules (optical methods), however, a broad range of experimental techniques can be used to probe vibrations at surfaces. Methods based on electron scattering (EELS), neutral atom scattering, infrared reflectance, Raman spectroscopy and inelastic tunneling are in widespread use. Each of these techniques has limitations and assets which have been discussed in various review papers.[7,8] Here, we will be concerned with the application of electron scattering to study surface vibrations.

It is now well-established that two distinct scattering regimes are required to account for experimental observations of vibrational losses measured by inelastic electron scattering from surfaces. The basic difference between these two regimes is that one is based on long-range dipolar fields which produce small-angle (forward) inelastic scattering, and the other is based on short-range atomic-like fields which produce large-angle (diffuse) inelastic scattering.

Vibrational losses observed using specular geometry (equal incident and scattering angles) generally result from the "dipole" scattering mechanism.[9] In this scattering regime, the process is viewed as a combination of inelastic forward scattering by dipolar fields followed or preceded by elastic backscattering (reflection) from the surface. Dipole scattering is therefore characterized by a narrow spread around the specular scattering angle.

A second and distinctly different scattering regime termed "impact"

scattering[10] is associated with short-ranged atomic-like potentials. Electrons scattered by vibrational excitations in this regime exhibit a much more isotropic angular spread.[11] In addition, the cross-section energy dependence is no longer a simple decreasing monotonic function of $E_i$, as is the case for dipole scattering, and in fact contains structure which is related to bond distances and other geometrical parameters.[10] The most striking difference between these two scattering mechanisms from an experimental point of view is the relative magnitude of the differential scattering cross sections. The total scattering cross section for impact scattering is comparable to (or larger than) dipole cross sections. However, under typical experimental conditions, when the energy analyzer defines a small acceptance cone (typically $\Delta\Omega$ is $1^o$ or less), the actual counting rate associated with the two scattering mechanisms is vastly different. For example, with a clean, well-ordered crystal, state-of-the-art EELS spectrometers operating at 5meV resolution yield elastic peak counting rates in specular geometry of about $10^5$ Hz. A dipole loss feature of monolayer coverages will yield typical counting rates, under the same conditions, of a few hundred Hz, and an impact loss peak, observed under corresponding conditions, will yield a counting rate of the order of 1 Hz or less.

The extremely low counting rates encountered in studying vibrational losses using the impact scattering regime help explain the fact that very few EELS experiments have been conducted using off-specular scattering geometry. New instrumentation is currently being developed which should improve the counting rates by a factor of approximately 100. There are several good reasons for attempting to achieve a major improvement in the capability of EELS spectrometers to determine impact scattering cross sections. Some of these will be clear from the following discussion.

Energy and momentum conservation laws associated with the excitation of a phonon of energy $\hbar\omega$ by an electron require

$$E_i = E_s + \hbar\omega \tag{1}$$

$$\vec{k}_i \sin\theta_i = \vec{k}_s \sin\theta_s + \vec{q}_{11} + \vec{G}_{11} \tag{2}$$

where $\vec{G}_{\parallel}$ is a two-dimensional lattice vector (usually 0) and $\vec{q}_{\parallel}$, the momentum transfer parallel to the surface, is restricted to the first Brillouin zone. These equations show that electron scattering from a surface can be regarded as the two-dimensional analog of the well-known thermal neutron studies of bulk phonons. The impact scattering mechanism allows losses to be detected when $\theta_s \neq \theta_i$ (i.e. in off-specular scattering geometry) and the $\vec{q}_{\parallel}$ dependence of the loss can be determined by solving Eq. (2):

$$|\vec{q}_{\parallel}| = \frac{2m_e}{\hbar} \left| \sqrt{E_i}\sin\theta_i - \sqrt{E_s - \hbar\omega}\,\sin\theta_s \right| \tag{3}$$

Evaluation of Eq. 3 for a few relevant values of $\vec{q}_{\parallel}$ ($1\text{-}2\text{Å}^{-1}$) shows that in order to cover the two-dimensional Brillouin zone, incident energies of the order of 250 eV are required. Impact energies in the 200-300 eV range are also convenient for another reason: dipole scattering cross-sections decrease with increasing impact energy and higher impact energies help discriminate against dipole losses when working near the specular direction.

## III. Experimental Results

Having briefly described some features of electron scattering from surfaces which have bearing on the study of surface vibrations, we now consider two

examples where such studies have yielded new insight into the surface structure and properties. Both examples are based on combining the results of EELS measurements with lattice dynamical calculations to address issues related to molecular level surface geometry.

a) O/Al(111)

Our study of the initial stage of oxide formation on Al(111) was stimulated by the apparent confusion regarding O-Al bond distances and the location of oxygen atoms at low coverages, (1x1)O/Al(111), as determined by low-energy electron diffraction (LEED) and other structural techniques.[1,2] Workfunction[12] and photoemission[13] measurements had also suggested an instability in the surface complex which formed at room temperature, and EELS appeared to offer a new and independent method for studying the systems.

Figure 1 displays EELS spectra for (1x1)O/Al(111) for several doses before and after annealing the sample. These spectra immediately accounted for a major part of the problems encountered in LEED studies[14] which had attempted to determine the O-Al bond distance. The EELS spectra indicate that a mixed phase forms which consists of both underlayer and overlayer sites of the Al lattice being occupied by oxygen atoms. The instability of the oxygen overlayer, as indicated by previous workfunction[12] and photoemission[13] results was also apparent from the time-dependent change in EELS loss peak intensities which occurred at room temperature and from the accelerated changes which occurred at higher temperatures.

Assignment of the loss peaks to phonon modes involving both overlayer and underlayer oxygen atoms in various high-symmetry configurations of the Al(111) lattice (refer to the inset of Fig. 1) were verified using lattice dynamical calculations.[2] In these calculations, the Al lattice was modeled using central forces based on Lennard-Jones potentials and O-O and O-Al interactions were also

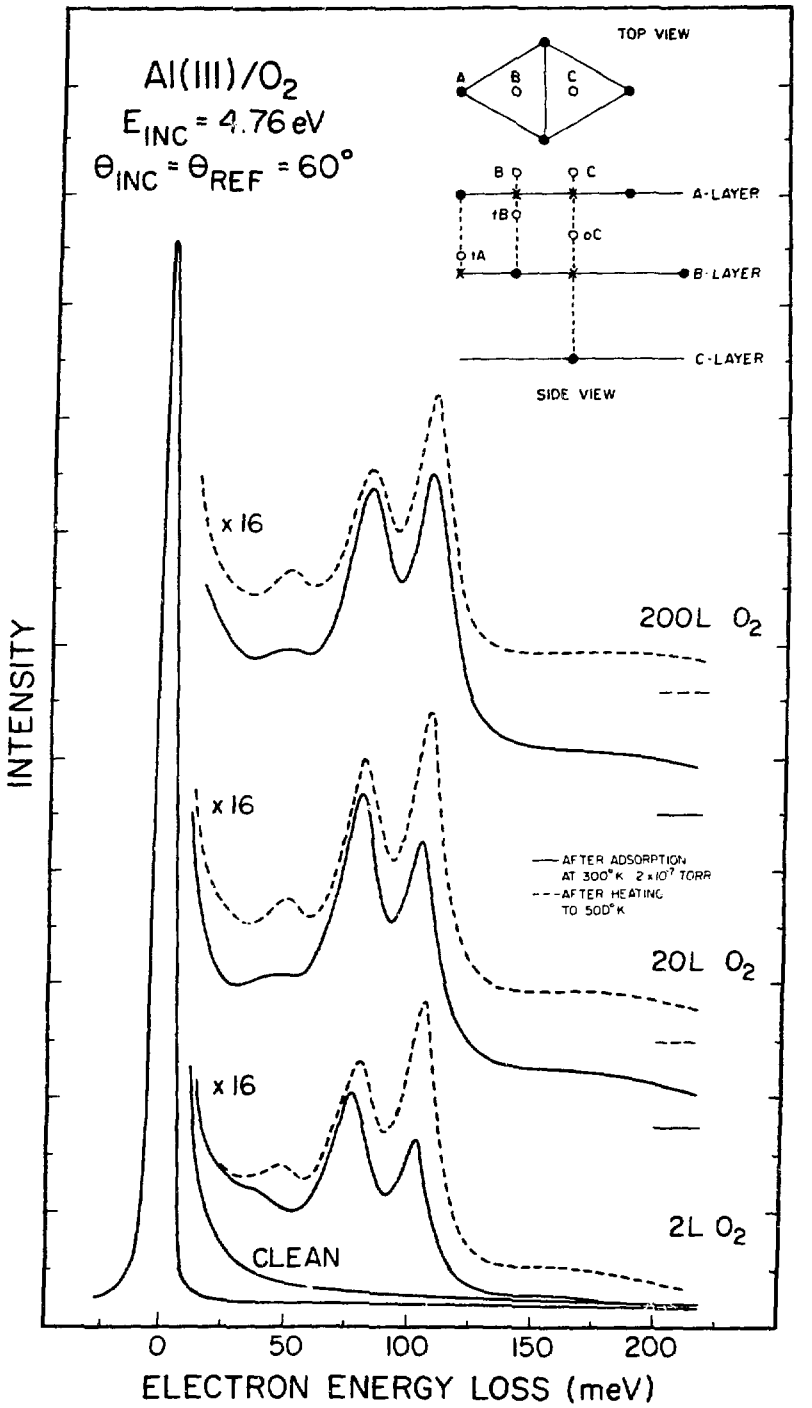


Figure 1 EELS spectra for 2, 20, and 200 L (1L = $10^{-6}$ Torr sec) $O_2$ on Al(111) before and after annealing. The 80-meV peak corresponds to surface oxygen and the 105-meV peak corresponds to subsurface oxygen, and the 105 meV peak results from coupling of first and second Al layers through the subsurface oxygen. Inset: lattice model for the Al(111) surface showing possible positions for overlayer (B and C) and underlayer (tB, tA and Oc) oxygen atoms.

treated using central force constant parameters. Based on the established lattice symmetry, six distinct configurations of surface and subsurface oxygen atoms at the Al(111) surface were allowed (by the (1x1) LEED patterns observed for this system) and the lattice dynamical models were able to eliminate all possibilities except two. Overlayer/underlayer configurations yielding vibrational modes which could not be reconciled with energies and polarization of the three vibrational bands determined experimentally were rejected as possible configurations. The lattice calculation predicted that the underlayer oxygen occupies the tB site, and that the overlayer oxygen occupied the C site illustrated in the inset of Fig. 1.

This study represents one of the first direct applications of EELS combined with lattice dynamical calculations to investigate a structural property of a surface adsorbate complex.

b) O/Ni(100)

We have also investigated the vibrational properties of clean Ni(100), and two ordered overlayer systems (p(2x2) and c(2x2)) of O on Ni(100). The O/Ni(100) system is particularly interesting because of the large number of investigations which have been carried out, and although many of the uncertainties which have arisen from these studies now seem to have been settled, there remain a few questions to be addressed. It would be very difficult to consider all of the work on this system within the context of the present discussion, which is concerned with how EELS can be used to address structural questions, and therefore, only a carefully selected subset of related work is described in the following brief historical account.

The binding distance of O on Ni(100) has been one of the more controversial issues in the field of surface crystallography. LEED studies[15] have determined

that c(2x2) and p(2x2) chalcogens (including oxygen) bind at the four-fold hollow site, and for both c(2x2) and p(2x2) overlayers of Te, Se, and S, the LEED determined $d_\perp$ spacings have been well-corroborated by other spectroscopic techniques and by ab initio calculations. This is not the case for c(2x2) and p(2x2) O overlayers.

While the original $d_\perp$ value for p(2x2) O/Ni(100) determined by LEED ($d_\perp$=0.9,Å) appears to have held up, the corresponding result for c(2x2) (which is also $d_\perp$=0.9Å) has been challenged by subsequent studies[16] (including LEED), and corroborated by others.[17-20] One of the more recent LEED papers[17] summarizes the conclusions drawn by investigators using a number of techniques which include ion scattering[19] ($d_\perp$=0.9Å), photoelectron diffraction[20] ($d_\perp$=0.9Å or 0.0Å depending on coverage), and lattice dynamical calculations[22] (d=0.27Å) which were based on cluster calculation derived potential energy curves.[23] The LEED paper[17] reports that there is no <u>improved</u> agreement between calculated I-V curves and extensive experimental data for any value of $d_\perp$ other than the original value of 0.9Å, however, $d_\perp$ values $\lesssim$ 0.1Å exhibit roughly the same fit. The most recent LEED paper on the subject[24] suggests that $d_\perp$=0.80Å and that the oxygen atom is displaced 0.30Å from the fourfold hollow position along a <110> direction. The new structure is called a pseudo-bridge bond which corresponds to $C_{2v}$ symmetry and yields two inequivalent nearest-neighbor Ni-O bond distances of 1.75 Å and 2.14 Å. The remainder of this paper discusses some of our efforts to resolve these discrepancies using EELS and lattice dynamical calculations.

Figure 2 illustrates a particular calculation of surface phonon bands along the $\bar{\Gamma}$-$\bar{X}$ direction of the two-dimensional Brillouin zone of c(2x2)O/Ni(100).[25] The calculation is based on a 13-layer face-centered-cubic slab with (100) orientation of the surface planes.[2] All force constants in the model are assumed

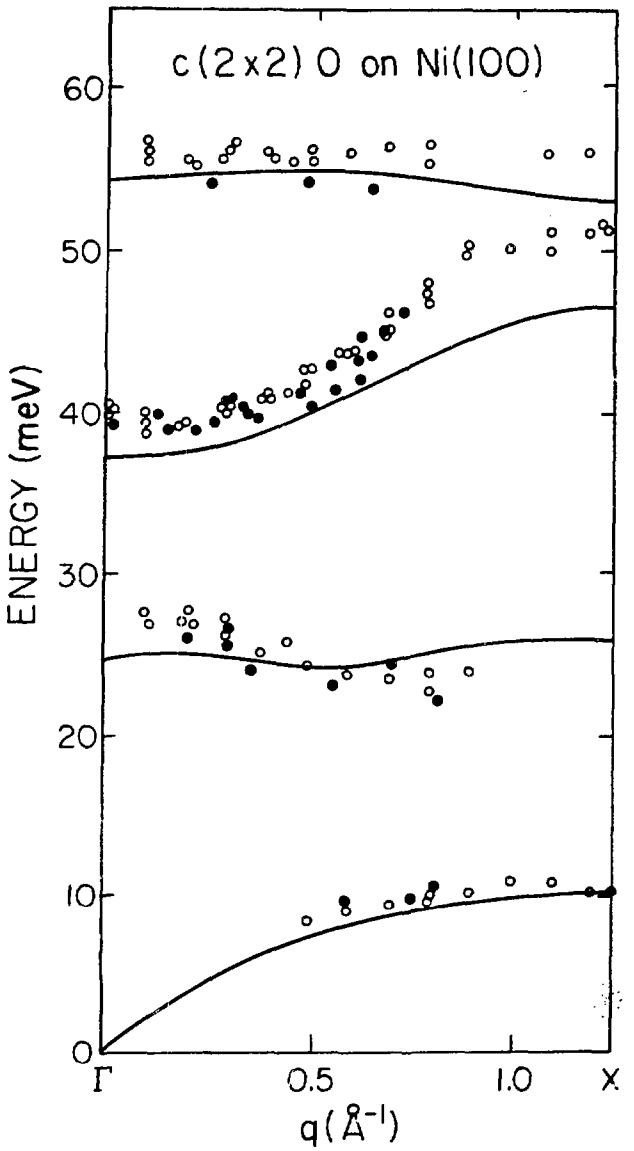


Figure 2 Calculated surface phonon bands along the $\bar{\Gamma}$-$\bar{X}$ direction of the two-dimensional Brillouin zone of c(2x2) O/Ni(100). Parameters used in the calculation are given in Table 1. Open circles, experimental data by Szeftel et al. (ref. 4), solid circles, experimental data by Strong and Erskine (ref. 6).

to be described by central pair potentials of the Lennard-Jones type:

$$U(r) = 4\varepsilon[(\frac{\sigma}{r})^{12} - (\frac{\sigma}{r})^{6}] \ . \qquad (4)$$

The parameters we have used to obtain the particular phonon bands in Fig. 2 are listed in Table 1.

We have performed many similar calculations in which the parameters $\varepsilon$, $\sigma$ and the height $d_\perp$ have been varied. The objective of these calculations is to

| | $\varepsilon$ | $\sigma$ |
|---|---|---|
| Bulk Nickel | 1.375 | 0.8909 |
| Layer 1 - Layer 1 | 1.553 | 0.8909 |
| Layer 1 - Layer 2 | 0.375 | 0.9143 |
| Layer 1 - Layer 2 | 2.192 | 0.7134 |
| Oxygen - Oxygen | 0.555 | 1.2599 |

Table 1 Lennard-Jones parameters for best fit to EELS data (at $k_{11} = 0.3\text{Å}^{-1}$ and $0.8\text{Å}^{-1}$) for c(2x2) oxygen on Ni(100). The $d_\perp$ value for oxygen is 0.922Å. This model assumes only nearest-neighbor interactions, with no anglebending forces and a 5.2% relaxation of the first Ni layer.

determine the influence of parameter variations on the phonon bands in relation to experimental results. Also shown in Fig. 2 are results of our EELS measurements, and measurements by others, which establish the vibrational energies of adsorbate and substrate phonon bands.

We find that $d_\perp$ values of approximately 0.9Å yield the best fit with experimental phonon energies throughout the two-dimensional Brillouin zone, and that there does not appear to be a range of $d_\perp$ values in the range of 0.0Å to 0.2Å which yields an acceptable fit to data.

Finally, we have also investigated the effect of introducing a pseudo-bridge site oxygen with parameters as determined by the most recent LEED results, namely, $d_\perp = 0.08\text{Å}$ and $d_{11} = 0.3\text{Å}$ from the four-fold location. The effect of this geometry is to remove the degeneracy of the parallel modes (x and y directions are no longer equivalent). The splitting of the x- and y modes predicted by the calculation (using $\sigma$ and $\varepsilon$ parameters which yield good fits for the fourfold site) is approximately 4 meV. This splitting could be detected by EELS using scattering selectron rules provided that a single chemisorbed domain of $C_{2v}$ symmetry were formed on the surface. If patches of two different domains form, the x and y modes could not be separated using scattering selectron rules. and the observed result would be a broadening of the spectral features. It would be difficult to characterize the broadening well enough to imply a pseudo-bridge geometry for the c(2x2) O/Ni(100) system.

## IV. Summary

From these two examples, it appears that surface vibrational properties can be used to obtain information about surface geometry. The technique needs to be tested using several cases where geometry is already well-established by LEED, photoelectron diffraction and other structural probes. The two cases discussed here represent situations where LEED alone appears to have been inadequate for surface structure determination, and combined use of LEED, lattice dynamical models and vibrational spectroscopy has been necessary to arrive at the correct structural model.

Additional applications of the EELS technique to surface geometry have been suggested by recent theoretical studies which show that multiple-scattering enters into the description of the energy and angle dependent inelastic cross sections. The development of new EELS instruments will soon permit more rapid and accurate measurements of impact scattering cross-sections. These instruments will permit detailed studies of energy and angle dependencies in inelastic electron scattering cross-sections in the impact scattering regime.[10,26] Selection rules[10] related to surface geometry can be tested and measured cross-sections can be compared with calculations to determine the extent EELS can be used as a direct structural probe analogous to LEED. The advanced spectrometers may also permit dynamical (time-dependent) processes to be studied by analysis of the time evolution of vibrational bands of surface intermediates. Surface vibrational spectroscopy using electron scattering has come a long way since the pioneering work of Propst and Piper,[27] but it appears that there are many challenges remaining for instrument development, new applications and advancing our basic understanding of the phenomena.

Acknowledgment: This work was sponsored by the Air Force Office of Scientific Research, Grant No. AFOSR-83-0131.

## References


1. J. L. Erskine and R. L. Strong, Phys. Rev. B25, 5547 (1982).

2. R. L. Strong, B. Firey, F. W. deWette and J. L. Erskine, Phys. Rev. B26, 3483 (1982).

3. S. Lehwald, J. Szeftel, H. Ibach, T. S. Rahman and D. L. Mills, Phys. Rev. Letters 50, 518 (1983).

4. J. Szeftel, S. Lehwald, H. Ibach, T. S. Rahman, J. E. Black and D. L. Mills, Phys. Rev. Letters 51, 268 (1983).

5. T. S. Rahman, J. E. Black and D. L. Mills, Phys. Rev. B25, 883 (1982).

6. R. L. Strong and J. L. Erskine, (to be published).

7. G. T. Haller, Catal. Rev. Sci. Eng. 23, 477 (1981).

8. H. Ibach, Proc. of the 7th International Vacuum Congress and Third International Conference on Solid Surfaces, Vienna (1977).

9. E. Evans and D. L. Mills, Phys. Rev. B5, 4126 (1972); B7, 853 (1973).

10. S. Y. Tong, C.-H. Li and D. L. Mills, Phys. Rev. Letters 44, 407 (1980); Phys. Rev. B24, 806 (1981).

11. W. Ho, R. F. Willis and E. W. Plummer, Phys. Rev. B21, 4202 (1980).

12. P. O. Gartland, Surf. Sci. 62, 183 (1979); P. Hofmann, W. Wyrobisch and A. M. Bradshaw, Surf. Sci. 80, 344 (1979); R. Michel, J. Gastaldi, C. Allasia and C. Jordan, Surf. Sci. 95, 309 (1980).

13. P. Hofmann, W. Wyrobisch and A. M. Bradshaw, Surf. Sci. 80, 344 (1980); P. Hofmann, C. Munschwitz, K. Horn, K. Jacobi, A. M. Bradshaw and K. Kambe, Surf. Sci. 89, 322 (1979).

14. H. L. Yu, M. C. Munoz, and F. Soria, Surf. Sci. 94, L184 (1980); C. W. B. Martinson, S. A. Flodstrom, J. Rundgren and P. Westrim, Surf. Sci. 89, 102 (1979); R. Payling and J. A. Ramsey, J. Phys. C13, 505 (1980); F. Soria, V. Martinez, M. C. Munoz and J. L. Sacedon, Phys. Rev. B24, 6926 (1981).

15. J. E. Demuth, D. W. Jepsen and P. M. Marcus, Phys. Rev. Lett. 31, 540 (1973); M. A. Van Hove and S. Y. Tong, J. Vac. Sci. Technol. 12, 230 (1975).

16. S. Andersson, B. Kasemo, J. B. Pendry, and M. A. Van Hove, Phys. Rev. Lett. 31, 595 (1973); C. B. Duke, N. O. Lipan, and G. E. Laramore, Nuovo cimento 23B, 241 (1974).

17. S. Y. Tong and K. H. Lau, Phys. Rev. B25, 7382 (1982).

18. G. Hanke, E. Lang, K. Heinz and K. Müller, Surf. Sci. 91, 551 (1980).

19. H. H. Brongersma and J. B. Theeten, Surf. Sci. 54, 519 (1976).

20. D. H. Rosenblatt, J. C. Tobin, M. G. Mason, R. F. Davie, S. D. Kevan, D. A. Shirley, C. H. Li and S. Y. Tong, Phys. Rev. B23, 3828 (1981).

21. T. S. Rahman, J. E. Black and D. L. Mills, Phys. Rev. Lett. 46, 1469 (1981).

22. T. H. Upton and W. A. Goddard III, Phys. Rev. Lett. 46, 1635 (1981).

23. J. E. Demuth, N. J. DiNardo and G. S. Gargill III, Phys. Rev. Lett. 50, 1373 (1983).

24. R. L. Strong and J. L. Erskine (to be published).

25. G. C. Aers, T. B. Grimley, J. B. Pendry and K. L. Sebastian, J. Phys. C: Solid State Phys. 14, 3995 (1981).

26. F. M. Propst and T. C. Piper, J. Vac. Sci. Technol. 4, 53 (1967).